

Study of the Power Performance of GaN Based HEMTs with varying Field Plate Lengths

Gokhan Kurt, Ahmet Toprak, Ozlem A. Sen, and Ekmel Ozbay

Abstract—In this paper, we report the optimum power performance of GaN based high-electron-mobility-transistors (HEMTs) on SiC substrate with the field plates of various dimensions. The AlGaIn/GaN HEMTs are fabricated with 0.6 μm gate length, 3 μm drain-source space. And also, the field plate structures with the lengths of 0.2, 0.3, 0.5, and 0.7 μm have been fabricated on these HEMTs. Great enhancement in radio frequency (RF) output power density was achieved with acceptable compromise in small signal gain. A HEMT of 0.5 μm field plate length and 800 μm gate width is biased under 35 V, at 3 dB gain compression, The results showed that we obtained a continuous wave output power of 36.2 dBm (5.2 W/mm), power-added efficiency (PAE) of 33% and a small signal gain of 11.4 dB from this device. We also could achieve a continuous wave output power of 37.2 dBm (5.2 W/mm), power-added efficiency (PAE) of 33.7% and a small gain of 10.7 dB from another HEMT with 0.5 μm field plate length and 1000 μm gate width. These results were obtained at 8 GHz without using a via hole technology. The results seem very stunning in this respect.

Keywords—Field Plate, GaN HEMT, RF power applications, coplanar waveguide, power amplifiers

I. INTRODUCTION

HIGH electron mobility transistors have always been one of the most attracting field of interest because of their outstanding properties comparing the other field effect transistors in microelectronic industry. There have been made numerous theoretical and practical studies so far [1]-[3]. However Gallium Nitride (GaN) based high-electron-mobility-transistor (HEMT) devices are of great interest for high radio frequency (RF) power applications due to highly demanded

This work is supported by the projects DPT-HAMIT, DPT-FOTON, NATO-SET-193 and TUBITAK under Project Nos., 113E331, 109A015, 109E301. One of the authors (E.O.) also acknowledges partial support from the Turkish Academy of Sciences.

Gokhan Kurt is with the Nanotechnology Research Center-NANOTAM, Bilkent University, 06800 Ankara, TURKEY (phone: +90530-908-3562; fax: +90312-266-40-42; e-mail: gokurt@bilkent.edu.tr).

Ahmet Toprak is with the Nanotechnology Research Center-NANOTAM, Bilkent University, and 06800 Ankara, TURKEY (e-mail: atoprak@bilkent.edu.tr).

Ozlem A. Sen, is with the Nanotechnology Research Center-NANOTAM, Bilkent University, 06800 Ankara, TURKEY (e-mail: ozlem@bilkent.edu.tr).

Ekmel Ozbay is with the Nanotechnology Research Center-NANOTAM, Bilkent University, 06800 Ankara, TURKEY, Department of Electrical and Electronics Engineering, Bilkent University, 06800 Ankara, TURKEY and Department of Physics, Bilkent University, 06800 Ankara, TURKEY (e-mail: ozbay@bilkent.edu.tr)

physical and electrical properties of AlGaIn/GaN HEMTs offer far superior features such as high current density, high breakdown voltage, high thermal conductivity and high saturation velocity compared to gallium arsenide (GaAs) based HEMTs. Although, there is significant work on GaN HEMTs using field plates with very high output power densities for micro strip line (MSL) passive technology [4]-[7], yet to date, there have been only few reports on the effect of field plate length on HEMTs without via-hole technology, i.e. HEMTs suitable for coplanar waveguide (CPW) passive technology [8]. In this work, a systematic study of the effect of field plate dimensions on small signal gain, power, efficiency and cut off frequency is presented. GaN-HEMTs are fabricated with different field plate lengths. All the field plate structures are deployed in the vicinity of the gate contacts on the Si_3N_4 dielectric passivation layer. The electric field modification that is because of the field plates helps to smooth the peak value of the electric field on the channel caused by gate contact at the drain side of the gate edge. Thus it improves the breakdown voltage and the power performance of the HEMT. The benefit is also a reduced high-field trapping effect. As the field plate functions by reducing the electric field at the edge of the gate on the drain side, it prevents electron emission and electron trapping. As a result it helps the reduction of the current collapse effect of the transistors. In addition to power performance, field plate structures have also impact on the noise performance of HEMTs.

The performances of HEMTs with six and eight gate fingers are measured. The gate dimensions of the measured HEMTs are 0.6 $\mu\text{m} \times 6 \times 125 \mu\text{m}$ and 0.6 $\mu\text{m} \times 8 \times 125 \mu\text{m}$ and average gate-to-gate distance is 60 μm (Fig. 1). The schematic of the designed HEMT (0.6 $\mu\text{m} \times 6 \times 125 \mu\text{m}$) is given in Fig. 2. In this schematic, L_{gs} is 0.7 μm , L_g is 0.6 μm , L_{gd} is 1.7 μm and four different field plate lengths are designed as 0.2 μm , 0.3 μm , 0.5 μm and 0.7 μm . The thickness of the Si_3N_4 dielectric passivation layer is 300 nm.

II. DEVICE REALIZATION

AlGaIn/GaN HEMT epitaxial structure was grown on a semi-insulating SiC substrate by metal organic chemical vapor deposition. The structure consists of, 15 nm-thick AlN nucleation layer, a 2 μm -thick undoped GaN buffer layer, an approximately 1.5 nm-thick AlN interlayer, a 20 nm-thick undoped $\text{Al}_{0.22}\text{Ga}_{0.78}\text{N}$ layer and a 2 nm-thick GaN cap layer on the top of the structure. Then the Hall mobility and the

sheet carrier concentration values are measured. The Hall mobility was $1384 \text{ cm}^2\text{V}^{-1}\text{s}^{-1}$ whereas the sheet carrier concentration was $1.51 \times 10^{13} \text{ cm}^{-2}$.

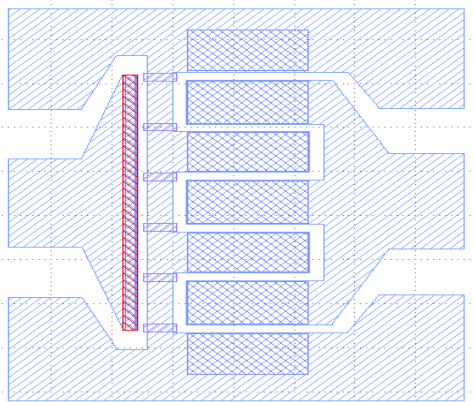


Fig. 1 Layout of the field-plated AlGaIn/GaN HEMT structure

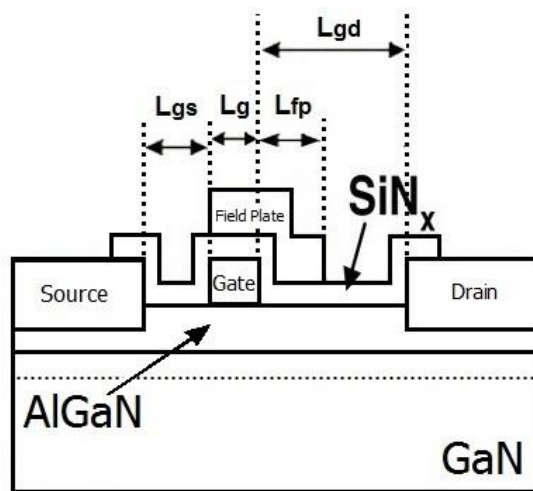


Fig. 2 Schematic of field-plated AlGaIn/GaN HEMT structure

Mesa etching was performed with ICP-RIE with a $\text{Cl}_2/\text{BCl}_3/\text{Ar}$ gas mixture. Ohmic contacts formation was done by Ti/Al/Ni/Au metal stack with the thicknesses of 12 nm, 120 nm, 35 nm and 65 nm, respectively. Ohmic contact metals were deposited by e-beam evaporation method. They were annealed in nitrogen ambient at $850 \text{ }^\circ\text{C}$ for 30 s. After ohmic contacts had been formed, the TLM measurements were done. Ohmic contact resistance was $0.6 \text{ } \Omega\text{-mm}$ and the measured sheet resistance was $460 \text{ } \Omega\text{-}\square^{-1}$. Fabrication process flow diagram of the HEMTs is given in Fig. 3. Ni/Au was deposited for gate contacts and subsequently an intermediate DC test measurement was done in order to check on whether the fabrication is proceeding as it is planned beforehand. This on-wafer DC operation test measurement of the devices was done prior to Si_3N_4 dielectric passivation using an Agilent B1500A semiconductor device parameter analyzer. In this measurement, the peak extrinsic transconductance (g_m) value was 215 mS/mm and the maximum current density value was

875 mA/mm . As the next step in fabrication, the device was passivated with a 300 nm-thick Si_3N_4 layer grown by plasma-enhanced chemical vapor deposition. After the passivation, the openings, where the interconnect metal will be deposited on, were formed by means of dry etching of ICP-RIE with CHF_3 gas. Thereafter, the test transistors were used to have DC test measurements again. Hence, we could observe the development impact of dielectric passivation on the transistors with this second DC test measurement.

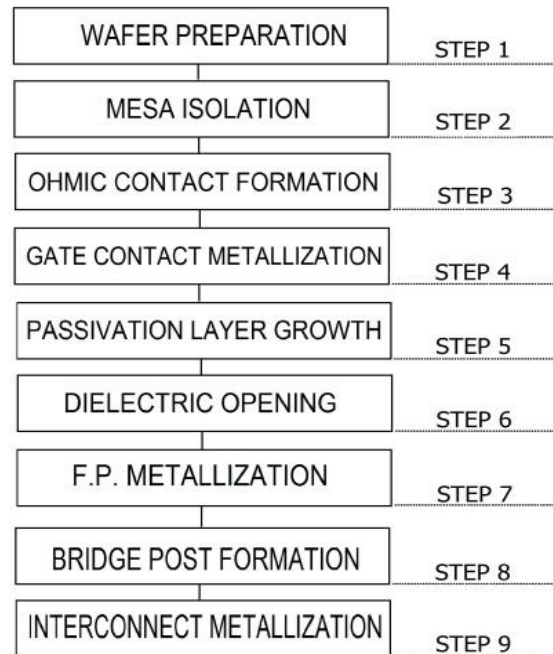


Fig. 3 Flow chart of GaN HEMT fabrication process including field plate step

After the passivation maximum current density was 1100 mA/mm and maximum extrinsic transconductance, g_m was 260 mS/mm . After this step, electron beam lithography is used to define the field plate regions and these regions were deposited with Ti/Au metals. The field plate structures were connected to the gate electrode with a gate bus. The air bridge post structures were constituted for preventing any case of being short circuit of the metals by functioning as a jumper. Finally, a relatively thick Ti/Au metal stack with e-beam evaporation had been deposited as an interconnection on the sample, and then the fabrication process was completed with this last step. Fig. 4 shows a $0.6 \times 6 \times 125 \text{ } \mu\text{m}$ HEMT's optical microscope image.

III. RESULTS AND DISCUSSIONS

DC on wafer measurements were performed using an Agilent B1500A semiconductor device parameter analyzer. For DC I-V characterization $0.6 \text{ } \mu\text{m} \times 2 \times 100 \text{ } \mu\text{m}$ the test transistor was used. The gates were biased from -4 to 1 V in a step of 1 V and drain current-voltage ($I_{\text{DS}}-V_{\text{DS}}$) characteristics is measured. The maximum current densities $I_{\text{ds, max}}$ for all

devices are nearly identical and around 1100 mA/mm except for the field plate length of 0.7 μm .

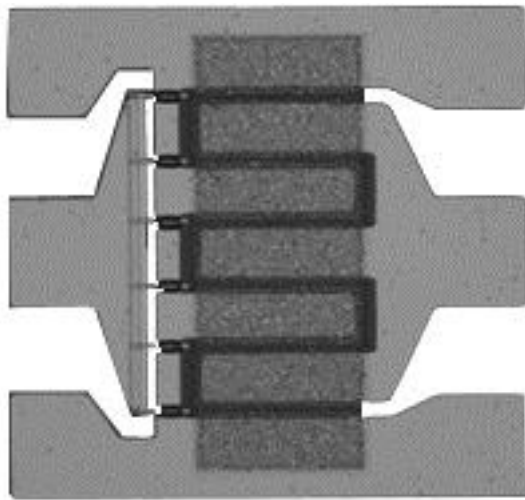


Fig. 4 Optical microscope image of fabricated $6 \times 125 \mu\text{m}$ HEMT

The measurement shows that for the device with $L_{fp} = 0.7 \mu\text{m}$, the current density drops since the distance between the field plate and the drain is smaller. The devices are completely pinched off at $V_{gs} = -4 \text{ V}$ and knee voltage is below 4 V which shows the excellence of ohmic contacts (Fig. 5).

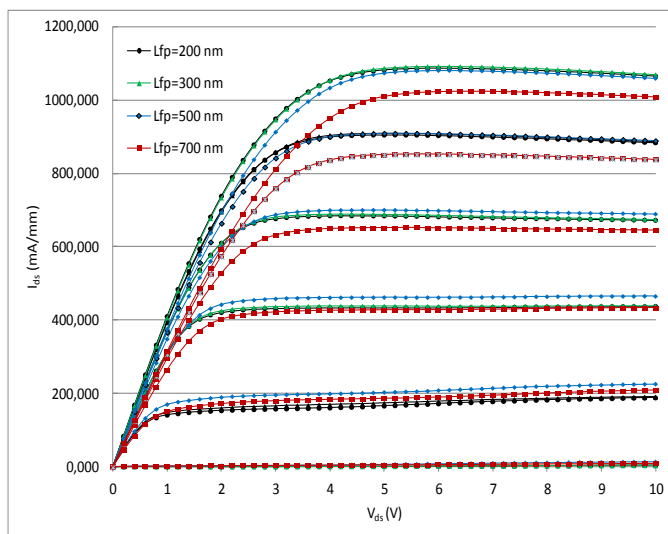


Fig. 5 Drain current-voltage ($I_{DS}-V_{DS}$) characteristics of a $0.6 \mu\text{m} \times 2 \times 100 \mu\text{m}$ AlGaIn/GaN HEMT with $L_{fp} = 0.2, 0.3, 0.5,$ and $0.7 \mu\text{m}$. The gate bias was swept from -4 to 1 V in a step of 1 V

In DC measurements, the extrinsic transconductance (g_m) is also measured. The peak transconductance value for all field plate lengths are above 250 mS/mm except for $L_{fp} = 0.7 \mu\text{m}$ and measured at $V_{gs} = -3.2 \text{ V}$. These results show that DC I-V transfer characteristics are independent of field plate length, the change in DC I-V transfer characteristics are due to the distance between field plate and drain contact, and in order not to decrease the current density and transconductance, this

distance should be higher than $1.1 \mu\text{m}$. Fig. 6 shows the transconductance (g_m-V_{gs}) characteristics of a $0.6 \mu\text{m} \times 2 \times 100 \mu\text{m}$ AlGaIn/GaN HEMT with $L_{fp} = 0.2, 0.3, 0.5,$ and $0.7 \mu\text{m}$.

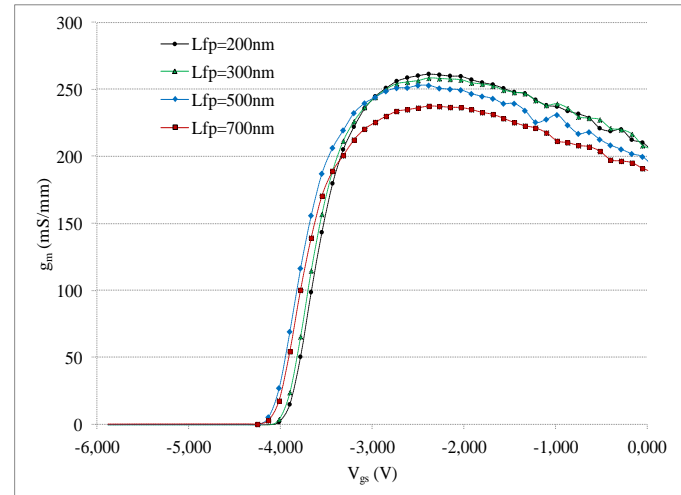


Fig. 6 Transconductance (g_m-V_{gs}) characteristics of a $0.6 \mu\text{m} \times 2 \times 100 \mu\text{m}$ AlGaIn/GaN HEMT with $L_{fp} = 0.2, 0.3, 0.5,$ and $0.7 \mu\text{m}$

On-wafer radio frequency (RF) measurements were carried out using a Cascade Microtech Probe and an Agilent E8361A PNA in the 1–20 GHz range. In small signal RF measurements the HEMTs with six fingers and with gate width of $6 \times 125 \mu\text{m}$ ($0.6 \mu\text{m} \times 6 \times 125 \mu\text{m}$) are used. Short-circuit current gain $|H_{21}|$ and Mason's unilateral power gain G_u derived from on-wafer S-parameter measurements as a function of frequency for the devices with field-plate length of 0.2, 0.3, 0.5 and 0.7 μm (Fig. 7). With these measurements, it was seen that, for all the field plate lengths, the unity current gain cut off frequency, f_t was above 20 GHz, and maximum oscillation frequency f_{max} was above 30 GHz. This is reasonable since the gate lengths of all the HEMTs are same. As the field plate length increases, the gate resistance decreases. But due to the 300-nm-thick Si_3N_4 passivation layer, the gate capacitances (especially C_{gd}) also increase. As a result, the change in f_{max} is negligible.

Large signal load pull measurement is carried on using Maury Microwave automated load pull system at 8 GHz. The data were taken on-wafer at room temperature without any thermal management. First of all, $0.6 \mu\text{m} \times 6 \times 125 \mu\text{m}$ HEMTs are measured at a drain bias of 35 V, and the output power, gain and power added efficiency (PAE) values are obtained (Fig. 8). The output power of the device with L_{fp} of 0.5 μm at 3dB gain compression is 5.2 W/mm with a PAE of 33% and a small signal gain of 11.4 dB at 8 GHz. Fig. 8 shows the large-signal performance of the $0.6 \mu\text{m} \times 6 \times 125 \mu\text{m}$ with $L_{fp} = 0.2, 0.3, 0.5,$ and $0.7 \mu\text{m}$ at 8 GHz.

At a drain bias of 35 V, power densities of 3.3, 4.7, 5.2 and 4.2 W/mm (@ 3 dB gain comp.) and small signal gain of 12.2, 11.6, 11.4, 11.2 dB were measured for devices with L_{fp} of 0.2, 0.3, 0.5 and 0.7 μm , respectively (Fig. 9).

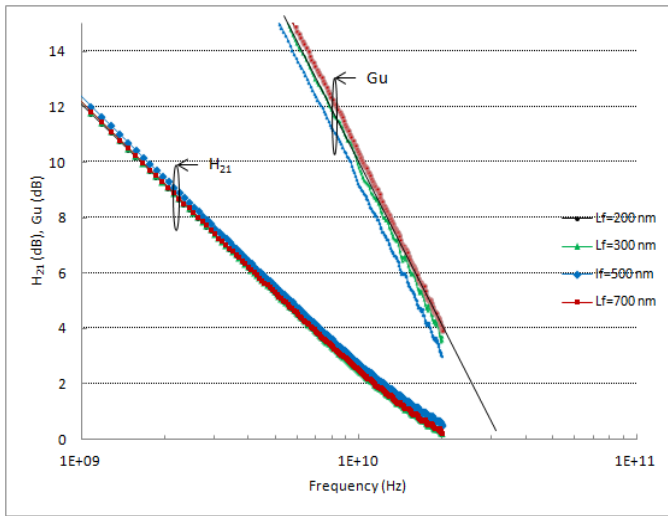


Fig. 7 Short-circuit current gain $|h_{21}|$ and unilateral power gain of a $0.6 \mu\text{m} \times 6 \times 125 \mu\text{m}$ AlGaIn/GaN HEMT with $L_{fp} = 0.2, 0.3, 0.5,$ and $0.7 \mu\text{m}$. Device was biased at $V_{DS} = 25 \text{ V}$ and $V_{gs} = -3.0 \text{ V}$

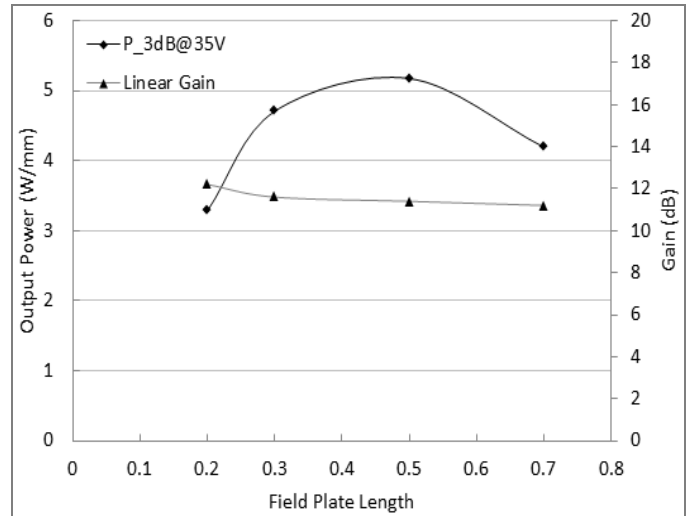


Fig. 9 Power performance versus length of field plate L_{fp} for devices of $0.6 \mu\text{m} \times 6 \times 125 \mu\text{m}$ when measured at 8 GHz with drain biases of 35 V

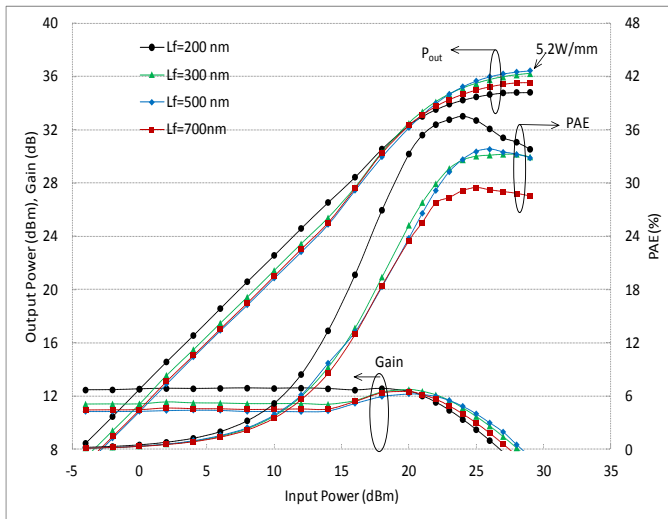


Fig. 8 Large-signal performance of the $0.6 \mu\text{m} \times 6 \times 125 \mu\text{m}$ with $L_{fp} = 0.2, 0.3, 0.5,$ and $0.7 \mu\text{m}$ at 8 GHz. The device was biased with $V_{ds} = 35 \text{ V}$ and $V_{gs} = -2.4 \text{ V}$

The DC, small signal and large signal results are summarized in TABLE I

TABLE I

Summary Of The Results Of The Field-Plated AlGaIn/GaN $0.6 \mu\text{m} \times 6 \times 125 \mu\text{m}$ HEMTs with Varying Field-Plate Length

L_{fp} (μm)	$g_{m,max}$ (mS/mm)	$I_{ds,max}$ (mA/mm)	f_t (GHz)	f_{max} (GHz)	Gain (dB)	Power (W/mm)
0.2	261	1080	20.2	32	12.2	3.3
0.3	259	1100	20.1	31	11.6	4.7
0.5	253	1080	20.3	30	11.4	5.2
0.7	237	975	20.2	31	11.2	4.2

From these results, it can be observed that, with the increase in field plate length, the output power density increases notably, with a negligible decrease in small signal gain unless the drain gate distance is above $1.1 \mu\text{m}$. When drain-gate distance is above $1.1 \mu\text{m}$, the parasitic capacitance C_{gd} increases and this capacitance limits the output power.

As a second power measurement, the HEMTs which they are able to give the highest power performance are measured under different drain bias voltages. $0.6 \mu\text{m} \times 8 \times 125 \mu\text{m}$ HEMTs with L_{fp} of $0.5 \mu\text{m}$ are measured at 25 V, 30 V, 32 V and 35 V drain bias. Output power values of 35.3 dBm, 36.4 dBm, and 36.9 dBm and, 36.6 dBm (@2 dB gain compression) and PAE of 43.7%, 37.8%, 36.9% and 33.6% were measured for devices with V_{DS} of 25, 30, 32 and 35 V (Fig. 10). Results are summarized in TABLE II.

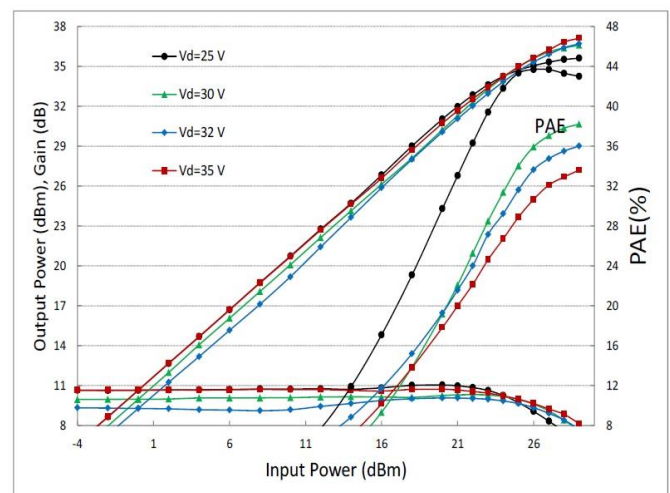


Fig. 10 Power performance versus drain bias V_{DS} for $0.6 \mu\text{m} \times 8 \times 125 \mu\text{m}$ with $L_{fp} 0.5 \mu\text{m}$ when measured at 8 GHz

TABLE II

Summary Of The Results Of The Field-Plated AlGaIn/GaN 0.8 μm \times 6 \times 125 μm HEMTs with L_{fp} 0.5 μm Varying V_{ds}

V_{DS}	Gain (dB)	Power (dBm) @ 2 dB comp	Power (W/mm) @ 2 dB comp	PAE (%)
25	10.6	35.3	3.4	43.7
30	9.9	36.4	4.35	37.8
32	9.3	36.9	4.9	36.9
35	10.6	36.6	4.6	33.6

These HEMTs will be used in X-band power amplifier application and the required frequency range is 8 - 12 GHz. So the large signal performances of these HEMTs are important. For this purpose, the large signal performance of the HEMTs with the best power and gain performance, i.e., $L_{fp} = 0.5 \mu\text{m}$, are measured at X-band frequencies. The data were taken on-wafer at room temperature without any thermal management. For 0.6 μm \times 8 \times 125 μm with $L_{fp} = 0.5 \mu\text{m}$, the output power at 8 GHz was above 36 dBm, but at 12 GHz the gain is too low to be used as a part of power amplifier (Fig. 11). In order to get enough gain at 12 GHz the device with six fingers (0.6 μm \times 6 \times 125 μm) is measured (Fig. 12). For the HEMT 0.6 μm \times 6 \times 125 μm with $V_{ds} = 30 \text{ V}$ and $V_{gs} = -2.4 \text{ V}$, at 12 GHz 33 dBm (2.67 W/mm) output power is obtained without any gain compression and with a gain of 8 dB. Since the input power of the measurement setup is limited at 12 GHz, the compression point is not measured but it was expected to be above 35 dBm (4.3 W/mm) at 3 dB gain compression. The measurement results given in Fig. 12 shows that the HEMT with 0.6 μm \times 6 \times 125 μm gate and $L_{fp} = 0.5 \mu\text{m}$ is suitable for the applications up to 12 GHz.

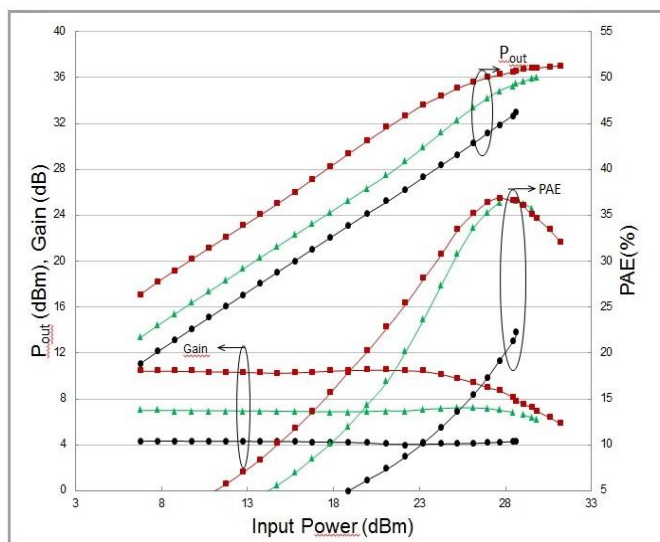


Fig. 11 Large-signal performance of the 0.6 μm \times 8 \times 125 μm with $L_{fp} = 0.5 \mu\text{m}$ at 8 GHz, 10 GHz and 12 GHz. The device was biased with $V_{ds} = 30 \text{ V}$ and $V_{gs} = -2.4 \text{ V}$

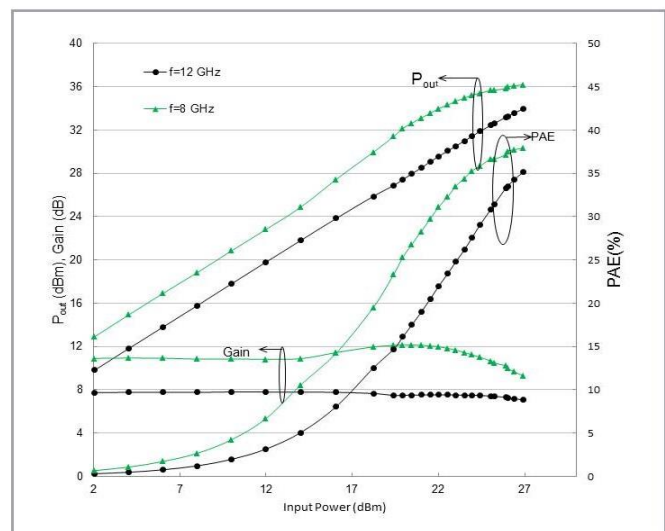


Fig. 12 Large-signal performance of the 0.6 μm \times 6 \times 125 μm with $L_{fp} = 0.5 \mu\text{m}$ at 8 GHz and 12 GHz. The device was biased with $V_{ds} = 30 \text{ V}$ and $V_{gs} = -2.4 \text{ V}$

IV. CONCLUSION

A systematic study has been performed to investigate the effect of a field plate on DC characteristics, small signal gain and large signal performance of GaN-channel HEMTs without via-hole technology. With 0.6 μm gate length, 300 nm-thick Si_3N_4 as a dielectric layer and 3 μm drain-source spacing, optimum field plate length was found to be 0.5 μm . These devices with field plate length of 0.2 μm , 0.3 μm and 0.5 μm exhibited high current densities of more than 1.0 A/mm and peak extrinsic transconductance values of more than 250 mS/mm. The DC I-V as well as transfer characteristics were essentially independent of the length of the field plate length. It was observed that when the space between the drain contact and the field plate decreases below 1.1 μm , the positive effect of the field plate on power densities are not observed.

With the increase of the field-plate length, degradation in the values small signal gain was observed, but there was significant improvement in power densities. Also, at 8 GHz, a CW output power density of 5.2 W/mm with PAE of 33% and a large signal gain of 8.2 dB at 3 dB gain compression at 8 GHz was obtained from a device with a field plate length of 0.5 μm without a via-hole technology. In addition, at 8 GHz, a CW output power of 36.9 dBm with PAE of 37% and a large signal gain of 8.4 dB at 2 dB gain compression at 8 GHz was obtained for 0.6 μm \times 8 \times 125 μm HEMTs at 32V drain-bias with a field plate length of 0.5 μm without a via-hole technology.

We aimed to make the fabrication of these high-electron-mobility-transistor devices for using them as the power amplifiers which they operate at X-band frequencies. Since they will be used in the 8-12 GHz frequency band, the power performances in this band were also examined. For this measurement, we used the devices with best power and gain performances. But, we see that the performance at 8 GHz

could not be obtained at 12 GHz from a device with the dimensions of $0.6 \mu\text{m} \times 8 \times 125 \mu\text{m}$ with $L_{fp} = 0.5 \mu\text{m}$. However from another device with six fingers ($0.6 \mu\text{m} \times 6 \times 125 \mu\text{m}$), 33 dBm (2.67 W/mm) output power is obtained without any gain compression and with a gain of 8 dB at 12 GHz.

In order to improve the power density performance, the drain-source spacing should be improved as a future work and then it would be possible to obtain larger field plate lengths without any degradation in power density values.

transistors, RF power and high frequency applications, GaN based HEMTs, micro-fabrication of micro-integrated circuits and transistors.

ACKNOWLEDGMENT

The authors would like to acknowledge Yildirim Durmus, Ogulcan Ariyurek, Pakize Demirel, Omer Cengiz, Orkun Arican, Huseyin Cakmak, Sinan Osmanoglu, Dogan Yilmaz, Burak Turhan and Ayca Emen for valuable support.

REFERENCES

- [1] R.Yahyazade, Z. Hashempour, G. Abdollahi, B. Baghdarghi, "Effect of High Temperature on the Transconductance of AlGaIn/GaN High Electron Mobility Transistors (HEMT)", *Proceedings of the 18th International Conference On Circuits (Part of CSCC'14), Advances Robotics, Mechatronics and Circuits*, 2014, pp 257-263.
- [2] F. Eshghabadi F. Banitorfian, M. Dousti, N. M. Noh, "A 2.4-GHz LNA: Design, Simulation, and Comparison in 0.2- μm GaAs p-HEMT Process and 0.35- μm SiGe BiCMOS HBT Process", *Proceedings of the 2013 International Conference on Electronics, Signal Processing and Communication Systems*, 2013.
- [3] T. Fernandez, F. Sanchez, M. Verdu, A. Tazon, A. Mimouni, J.A. Garcia, A. Mediavilla, "Modelling Reliability in GaN HEMT Devices", *8th WSEAS International Conference on Simulation, Modelling and Optimization (SMO '08)*, Santander, Cantabria, Spain, September 23-25, 2008.
- [4] U. K. Mishra, P. Parikh, Y. F. Wu, "AlGaIn/GaN HEMTs-an overview of device operation and applications", *Proceedings of the IEEE*, vol. 90, pp. 1022-1031, 2002.
- [5] Y.-F. Wu, A. Saxler, M. Moore, R. P. Smith, S. Sheppard, P. M. Chavarkar, T. Wisleder, U. K. Mishra, P. Parikh, "30-W/mm GaN HEMTs by Field Plate Optimization," *IEEE Electron Device Lett.*, vol. 25, pp. 117-119, March 2004.
- [6] V. Kumar, G. Chen, S. Guo, and I. Adesida, "Field-Plated 0.25- μm Gate-Length AlGaIn/GaN HEMTs With Varying Field-Plate Length," *IEEE Transactions on Electron Device*, vol. 53, pp. 1477-1480, June 2006.
- [7] Y. Ando, Y. Okamoto, H. Miamoto, T. Nakayama, T. Inoue, and M. Kuzuhara, "10 W/mm AlGaIn-GaN HFETs with a field modulating plate," *IEEE Electron Device Lett.*, vol. 24, no. 5, May 2003, pp. 289-291.
- [8] F. Van Raay, R. Quay, R. Kiefer, F. Benkhelifa, B. Raynor, W. Pletschen, M. Kuri, H. Massler, S. Müller, M. Dammann, M. Mikulla, M. Schlechtweg, G. Weimann, "A Coplanar X-Band AlGaIn/GaN Power Amplifier MMIC on s.i. SiC Substrate" *IEEE Microwave And Wireless Components Letters*, vol. 15, July 2005, pp.460-462.
- [9] G. Kurt, A. Toprak, O. A. Sen, E. Ozbay, "Effect of Field Plate Length on Power Performance of GaN Based HEMTs" *Proceedings of the 18th International Conference On Circuits (Part of CSCC'14), Advances Robotics, Mechatronics and Circuits*, 2014.

Corresponding Author: Gokhan KURT received the B.S. degree and the master's degree from the Department of Physics Engineering, Ankara University, Turkey in 2006. He is currently a Ph.D. candidate in the same department of Ankara University. He has also been working as a senior research engineer at Nanotechnology Research, Center of Bilkent University since 2009. His current research interests include RF and microwave Nano